

See discussions, stats, and author profiles for this publication at: <https://www.researchgate.net/publication/38087872>

Photophysics in Platinum(II) Bipyridylacetylides

ARTICLE *in* INORGANIC CHEMISTRY · NOVEMBER 2009

Impact Factor: 4.76 · DOI: 10.1021/ic901036a · Source: PubMed

CITATIONS

14

READS

30

5 AUTHORS, INCLUDING:



[Stéphane Diring](#)

University of Nantes

28 PUBLICATIONS 1,019 CITATIONS

SEE PROFILE

Photophysics in Platinum(II) Bipyridylacetylides

Maria L. Muro,[†] Stéphane Diring,[‡] Xianghuai Wang,[†] Raymond Ziessel,^{*,‡} and Felix N. Castellano^{*,†}

[†]Department of Chemistry and Center for Photochemical Sciences, Bowling Green State University, Bowling Green, Ohio 43403 and [‡]Laboratoire de Chimie Organique et Spectroscopies Avancées, associé au Centre National de la Recherche Scientifique (LCM-CNRS), Ecole de Chimie, Polymères, Matériaux (ECPM), 25 rue Becquerel, 67087 Strasbourg Cedex, France

Received May 28, 2009

The synthesis, structural characterization, photoluminescence, and excited state absorption properties of a series of platinum(II) terpyridyl complexes bearing a bipyridyl acetylide subunit are presented. The $[\text{Bu}_3\text{tpyPtC}\equiv\text{Cbpy}]^+$ (**1**) complex displays a broad and structureless emission profile at room temperature (RT), a lifetime of 5.8 μs , and transient absorption (TA) difference spectra characteristic of a charge transfer (CT) excited state. Upon coordination of Fe^{2+} to **1**, producing tetranuclear **2**, the CT emission was quantitatively quenched presumably through the low-lying iron-based ligand field states present. Surprisingly, the addition of Zn^{2+} to solutions of **1** produces a higher energy emissive state with a substantially longer excited state lifetime of 16.1 μs . The combined spectroscopic data measured for the zinc titration product (**3**) suggests that the overall excited state is dominated by a CT manifold, albeit at higher energy relative to **1**. The photophysics of a bis-phosphine complex bearing two *trans*-disposed bpy-acetylide subunits (**4**) produced a model chromophore possessing an intraligand triplet excited state with a lifetime of 26 μs at RT. The bipyridyl analogue of **1**, $[\text{Bu}_2\text{bpyPt}(\text{C}\equiv\text{Cbpy})_2]$ (**5**), was also prepared and its photophysics are consistent with a lowest CT parentage at RT. The 77 K emission spectra measured for complexes **1**, **3**, **4**, and **5** are all consistent with a triplet bpy-acetylide localized excited state; the E_{00} energies vary over a modest 344 cm^{-1} across the series. However, the shorter 77 K excited state lifetimes observed for **1**, **3**, and **5** in comparison to **4** suggests that the energetically proximate CT state in the former compounds significantly influences excited state decay at low temperature.

Introduction

The development of square planar platinum(II) complexes combining both polypyridyl and ancillary ligands such as acetylides have increased markedly over the past decade largely because of the impressive photophysical properties displayed by these compounds. The presence of low-energy absorption bands, long-lived excited states, high photoluminescence quantum yields have made platinum(II) polypyridyl complexes suitable for

comprehensive fundamental studies^{1–27} as well as for a variety of applications such as light-emitting materials,^{28,29}

*To whom correspondence should be addressed. E-mail: castell@bgsu.edu (F.N.C.), ziessel@unistra.fr (R.Z.).

(1) Castellano, F. N.; Pomestchenko, I. E.; Shikhova, E.; Hua, F.; Muro, M. L.; Rajapakse, N. *Coord. Chem. Rev.* **2006**, *250*, 1819–1828.

(2) Hissler, M.; McGarrah, J. E.; Connick, W. B.; Geiger, D. K.; Cummings, S. D.; Eisenberg, R. *Coord. Chem. Rev.* **2000**, *208*, 115–137.

(3) Williams, J. A. G. *Top. Curr. Chem.* **2007**, *281*, 205–268.

(4) Shikhova, E.; Danilov, E. O.; Kinayyigit, S.; Pomestchenko, I. E.; Tregubov, A. D.; Camerel, F.; Retaileau, P.; Ziessel, R.; Castellano, F. N. *Inorg. Chem.* **2007**, *46*, 3038–3048.

(5) Arena, G.; Calogero, G.; Campagna, S.; MonsuScolaro, L.; Ricevuto, V.; Romeo, R. *Inorg. Chem.* **1998**, *37*, 2763–2769.

(6) Crites, D. K.; Cunningham, C. T.; McMillin, D. R. *Inorg. Chim. Acta* **1998**, *273*, 346–353.

(7) Danilov, E. O.; Pomestchenko, I. E.; Kinayyigit, S.; Gentili, P. L.; Hissler, M.; Ziessel, R.; Castellano, F. N. *J. Phys. Chem. A* **2005**, *109*, 2465–2471.

(8) Hua, F.; Kinayyigit, S.; Cable, J. R.; Castellano, F. N. *Inorg. Chem.* **2005**, *44*, 471–473.

(9) Hua, F.; Kinayyigit, S.; Cable, J. R.; Castellano, F. N. *Inorg. Chem.* **2006**, *45*, 4304–4306.

(10) Hua, F.; Kinayyigit, S.; Rachford, A. A.; Shikhova, E. A.; Goeb, S.; Cable, J. R.; Adams, C. J.; Kirschbaum, K.; Pinkerton, A. A.; Castellano, F. N. *Inorg. Chem.* **2007**, *46*, 8771–8783.

(11) Whittle, C. E.; Weinstein, J. A.; George, M. W.; Schanze, K. S. *Inorg. Chem.* **2001**, *40*, 4053–4062.

(12) McMillin, D. R.; Moore, J. J. *Coord. Chem. Rev.* **2002**, *229*, 113–121.

(13) Michalec, J. F.; Bejune, S. A.; Cuttall, D. G.; Summerton, G. C.; Gertenbach, J. A.; Field, J. S.; Haines, R. J.; McMillin, D. R. *Inorg. Chem.* **2001**, *40*, 2193–2200.

(14) Michalec, J. F.; Bejune, S. A.; McMillin, D. R. *Inorg. Chem.* **2000**, *39*, 2708–2709.

(15) Moore, J. J.; Nash, J. J.; Fanwick, P. E.; McMillin, D. R. *Inorg. Chem.* **2002**, *41*, 6387–6396.

(16) Muro, M. L.; Castellano, F. N. *Dalton Trans.* **2007**, 4659–4665.

(17) Muro, M. L.; Diring, S.; Wang, X.; Ziessel, R.; Castellano, F. N. *Inorg. Chem.* **2008**, *47*, 6796–6803.

(18) Jude, H.; Bauer, J. A. K.; Connick, W. B. *Inorg. Chem.* **2004**, *43*, 725–733.

(19) Pomestchenko, I. E.; Castellano, F. N. *J. Phys. Chem. A* **2004**, *108*, 3485–3492.

(20) Rachford, A. A.; Goeb, S.; Ziessel, R.; Castellano, F. N. *Inorg. Chem.* **2008**, *47*, 4348–4355.

photocatalysis and hydrogen production,^{30–32} dye-sensitized solar cells,^{33,34} biosensors,^{35,36} photoswitches,³⁷ excited-state electron transfer,³⁸ singlet O₂ sensitization,^{16,17,39} vapochromism,^{40–47} and optical limiting materials.⁴⁸ A notable facet of the metal acetylide-bearing structures relates to the concept that their excited-state properties are easily tuned through alteration of the electronic structure of either the donor and/or the acceptor ligands appended to the Pt^{II} center.^{2,49–53}

The attachment of ancillary ligands possessing open coordination sites presents the possibility of generating new

polynuclear and polymetallic complexes with intriguing photophysical properties. Generally speaking, many Pt^{II} complexes studied to date can be considered end-capped, thereby limiting the possibility of structural expansion and hence the formation of more intricate supramolecular chromophores. Attachment of free-base pendant ligands to the Pt^{II} center will certainly open the possibility to generate heteronuclear complexes with the opportunity to study the resultant photophysical properties of these new polymetallic systems. The fact remains that only a handful of platinum(II) complexes carrying appended free ligands have been designed to date and include chelating moieties such as benzo-crown ethers,⁵⁴ terpyridine,¹⁷ and bipyridine.⁵⁵ Most of the resultant complexes have been used as metal ion or pH sensors because of the noticeable changes displayed in their absorption and emission properties upon coordination of the free pendant ligand(s) to ions present in the solution.

In previous work, we demonstrated that the photophysical properties of [^tBu₃tpyPtC≡Ctpy]⁺ are significantly influenced by chelation of either Zn^{II} or Fe^{II}; in the former case a higher energy CT excited state manifold was generated whereas quantitative quenching of the luminescence was observed in the latter.¹⁷ In the present study, the photophysical properties of a terpyridyl platinum(II) complex containing a pendant bipyridyl acetylide subunit [^tBu₃tpy-PtC≡Cbpy]⁺ (**1**) (where ^tBu₃tpy = 4,4',4''-tri-*tert*-butyl-2,2':6',2''-terpyridine) and its corresponding polynuclear Fe^{II} and Zn^{II} analogues, [Fe(^tBu₃tpyPtC≡Cbpy)₃]⁵⁺ (**2**), and [Zn(^tBu₃tpyPtC≡Cbpy)₃]⁵⁺ (**3**) are reported together with the photophysics of the phosphine model complex *trans*-(PEt₃)₂Pt(C≡Cbpy)₂ (**4**). The latter complex exhibits a bipyridyl centered lowest triplet excited state. For completeness, we also describe the photophysical properties of the bipyridyl platinum(II) analogue of **1**, ^tBu₂bpyPt(C≡Cbpy)₂ (**5**), where ^tBu₂bpy = 4,4'-di-*tert*-butyl-2,2'-bipyridine.

Experimental Section

General Procedures and Materials. [Pt(^tBu₃tpy)Cl]BF₄,²¹ 5-ethynyl-2,2'-bipyridine⁵⁶ and complex **5**⁵⁷ were prepared as described in the literature. Pt(dbbpy)Cl₂ was obtained according to a literature protocol.⁵⁸ [Pt(^tBu₃tpy)(C≡CPh)]ClO₄ (**6**) was available from a previous study.⁴ The synthon *trans*-[Pt-(Et₃P)₂Cl₂] was commercially available from Alfa Aesar and used as received. Fe(ClO₄)₂·6H₂O was obtained from Alfa Aesar and used without further purification. Zn(ClO₄)₂·6H₂O was purchased from Aldrich Chemical Co. and used as received. The titration experiments were carried out under an argon atmosphere, and the titrations were performed multiple times using freshly prepared solutions each time. A flow cell was used for the transient absorption measurements to prevent decomposition of the sample. All photophysical experiments were carried out with degassed CH₂Cl₂ solutions at room temperature. The transient absorption experiments with **4** were carried out in 2-methyltetrahydrofuran (MTHF) as this species was found to be unstable in CH₂Cl₂ under conditions of 2–3 mJ/pulse light fluence.

- (21) Yip, H.-K.; Cheng, L.-K.; Cheung, K.-K.; Che, C.-M. *J. Chem. Soc., Dalton Trans.* **1993**, 2933–2938.
- (22) Wong, K. M.-C.; Tang, W.-S.; Lu, X.-X.; Zhu, N.; Yam, V. W.-W. *Inorg. Chem.* **2005**, *44*, 1492–1498.
- (23) Muro, M. L.; Rachford, A. A.; Wang, X.; Castellano, F. N. *Top. Organomet. Chem.* **2009**, DOI: 10.1007/3418_2009_1.
- (24) Lee, S. J.; Luman, C. R.; Castellano, F. N.; Lin, W. *Chem. Commun.* **2003**, 2124–2125.
- (25) Pomestchenko, I. E.; Luman, C. R.; Hissler, M.; Ziessel, R.; Castellano, F. N. *Inorg. Chem.* **2003**, *42*, 1394–1396.
- (26) Goeb, S.; Rachford, A. A.; Castellano, F. N. *Chem. Commun.* **2008**, 814–816.
- (27) She, C.; Rachford, A. A.; Wang, X.; Goeb, S.; El-Ballouli, A. a. O.; Castellano, F. N.; Hupp, J. T. *Phys. Chem. Chem. Phys.* **2009**, *11*, 8586–8591.
- (28) Chan, S.-C.; Chan, M. C. W.; Wang, Y.; Che, C.-M.; Cheung, K.-K.; Zhu, N. *Chem.—Eur. J.* **2001**, *7*, 4180–4190.
- (29) Lu, W.; Mi, B.-X.; Chan, M. C. W.; Hui, Z.; Che, C.-M.; Zhu, N.; Lee, S.-T. *J. Am. Chem. Soc.* **2004**, *126*, 4958–4971.
- (30) Du, P.; Schneider, J.; Jarosz, P.; Eisenberg, R. *J. Am. Chem. Soc.* **2006**, *128*, 7726–7727.
- (31) Narayana-Prabhu, R.; Schmehl, R. H. *Inorg. Chem.* **2006**, *45*, 4319–4321.
- (32) Du, P.; Schneider, J.; Li, F.; Zhao, W.; Patel, U.; Castellano, F. N.; Eisenberg, R. *J. Am. Chem. Soc.* **2008**, *130*, 5056–5058.
- (33) Geary, E. A. M.; Yellowlees, L. J.; Jack, L. A.; Oswald, I. D. H.; Parsons, S.; Hirata, N.; Durrant, J. R.; Robertson, N. *Inorg. Chem.* **2005**, *44*, 242–250.
- (34) Islam, A.; Sugihara, H.; Hara, K.; Singh, L. P.; Katoh, R.; Yanagida, M.; Takahashi, Y.; Murata, S.; Arakawa, H.; Fujihashi, G. *Inorg. Chem.* **2001**, *40*, 5371–5380.
- (35) Ratilla, E. M. A.; Brothers, H. M.; Kostic, N. M. *J. Am. Chem. Soc.* **1987**, *109*, 4592–4599.
- (36) Wong, K. M.-C.; Tang, W.-S.; Chu, B. W.-K.; Zhu, N.; Yam, V. W.-W. *Organometallics* **2004**, *23*, 3459–3465.
- (37) Yutaka, T.; Mori, I.; Kurihara, M.; Mizutani, J.; Tamai, N.; Kawai, T.; Irie, M.; Nishihara, H. *Inorg. Chem.* **2002**, *41*, 7143–7150.
- (38) Cortes, M.; Carney, J. T.; Oppenheimer, J. D.; Downey, K. E.; Cummings, S. D. *Inorg. Chim. Acta* **2002**, *333*, 148–151.
- (39) Zhang, D.; Wu, L.-Z.; Yang, Q.-Z.; Li, X.-H.; Zhang, L.-P.; Tung, C.-H. *Org. Lett.* **2003**, *5*, 3221–3224.
- (40) Muro, M. L.; Daws, C. A.; Castellano, F. N. *Chem. Commun.* **2008**, 6134–6136.
- (41) Buss, C. E.; Anderson, C. E.; Pomije, M. K.; Lutz, C. M.; Britton, D.; Mann, K. R. *J. Am. Chem. Soc.* **1998**, *120*, 7783–7790.
- (42) Buss, C. E.; Mann, K. R. *J. Am. Chem. Soc.* **2002**, *124*, 1031–1039.
- (43) Exstrom, C. L.; Sowa, J. R. J.; Daws, C. A.; Janzen, D.; Mann, K. R.; Moore, G. A.; Stewart, F. F. *Chem. Mater.* **1995**, *7*, 15–17.
- (44) Grove, L. J.; Oliver, A. G.; Krause, J. A.; Connick, W. B. *Inorg. Chem.* **2008**, *47*, 1408–1410.
- (45) Grove, L. J.; Rennekamp, J. M.; Jude, H.; Connick, W. B. *J. Am. Chem. Soc.* **2004**, *126*, 1594–1595.
- (46) Wadas, T. J.; Wang, Q.-M.; Kim, Y.-j.; Flaschenreim, C.; Blanton, T. N.; Eisenberg, R. *J. Am. Chem. Soc.* **2004**, 16841–16849.
- (47) Du, P.; Schneider, J.; Brennessel, W. W.; Eisenberg, R. *Inorg. Chem.* **2008**, *47*, 69–77.
- (48) Guo, F.; Sun, W.; Liu, Y.; Schanze, K. *Inorg. Chem.* **2005**, *44*, 4055–4065.
- (49) McGarrah, J. E.; Eisenberg, R. *Inorg. Chem.* **2003**, *42*, 4355–4365.
- (50) McGarrah, J. E.; Kim, Y.-J.; Hissler, M.; Eisenberg, R. *Inorg. Chem.* **2001**, *40*, 4510–4511.
- (51) Du, P.; Schneider, J.; Jarosz, P.; Zhang, J.; Brennessel, W. W.; Eisenberg, R. *J. Phys. Chem. B* **2007**, *111*, 6887–6894.
- (52) Wadas, T. J.; Chakraborty, S.; Lachicotte, R. J.; Wang, Q.-M.; Eisenberg, R. *Inorg. Chem.* **2005**, *44*, 2628–2638.
- (53) Chakraborty, S.; Wadas, T. J.; Hester, H.; Flaschenreim, C.; Schmehl, R.; Eisenberg, R. *Inorg. Chem.* **2005**, *44*, 6284–6293.

(54) Tang, W.-S.; X.-X., L.; Wong, K. M.-C.; W.-W., Y. V. *J. Mater. Chem.* **2005**, *15*, 2714–2720.

(55) Diring, S.; Ziessel, R. *Tetrahedron Lett.* **2006**, *47*, 4687–4692.

(56) Grossshenny, V.; Romero, F. M.; Ziessel, R. *J. Org. Chem.* **1996**, *62*, 1491–1500.

(57) Ventura, B.; Barbieri, A.; Barigelletti, F.; Seneclauze, J. B.; Retailleau, P.; Ziessel, R. *Inorg. Chem.* **2008**, *47*, 7048–7058.

(58) Rendina, L. M.; Vittal, J. J.; Puddenphatt, R. *J. Organometallics* **1995**, *14*, 1030–1038.

Complex 1 was conveniently prepared from [Pt(^tBu₃tpy)-Cl]BF₄ (164 mg, 0.246 mmol), 5-ethynyl-2,2'-bipyridine (32 mg, 0.242 mmol), CuI (1.8 mg, 0.009 mmol), in DMF (3 mL), and triethylamine (1 mL) under strict anaerobic conditions, at room temperature (RT), during 21 h. During the course of the reaction, the color of the solution turned from yellow to deep-brown. After evaporation of the solvent, the residue was dissolved in a minimum DMF (about 3 mL), filtrated over Celite, and dropwise added to a stirred aqueous solution containing 50 equiv of NaBF₄. The formed precipitate was filtrated over paper, washed with water, and the solution was allowed to evaporate to dryness in a fume hood. Purification was carried out by chromatography on alumina, eluting with CH₂Cl₂-methanol (v/v 99/1) to CH₂Cl₂-methanol (v/v 97/3). Recrystallization by slow evaporation of dichloromethane from a solution containing dichloromethane/methanol afforded crystals of the desired complex as the BF₄ salt of **1** as an orange solid (82 mg, 76%). ¹H NMR (400.1 MHz, CDCl₃): δ 9.13 (d, ³J = 8.0 Hz, 2H), 8.96 (d, ³J = 8.2 Hz, 1H), 8.80 (d, ⁴J = 1.0 Hz, 1H), 8.67 (d, ³J = 6 Hz, 1H), 8.45 (s, 2H), 8.40–8.35 (m, 2H), 7.89 (dd, ³J = 8.0 Hz, ⁴J = 1.0 Hz, 1H), 7.84 (td, ³J = 8.0 Hz, ⁴J = 1.0 Hz, 1H), 7.66 (dd, ³J = 8.0 Hz, ⁴J = 2.0 Hz, 3H), 7.33–7.29 (m, 1H), 1.51 (s, 18H), 1.49 (s, 9H); ¹³C{¹H} NMR (100.6 MHz, CDCl₃+d₆-DMSO (v/v 1/1)): δ 162.4, 162.3, 157.9, 156.1, 155.7, 152.7, 150.7, 150.1, 140.1, 137.9, 125.3, 123.8, 123.7, 122.3, 121.6, 118.4, 114.7, 98.7, 41.4, 41.2, 31.7, 31.9; FT-IR (KBr, cm⁻¹): 2967, 2936, 2906, 2879, 2096 (ν_{C≡C}), 1586, 1567, 1537, 1457, 1432, 1411, 1376, 1363, 1269, 1252, 1205, 1149, 1093, 1052 (ν_{B-F}), 992, 940, 747; ES-MS *m/z* (nature of the peak, relative intensity): 775.2 ([M - BF₄]⁺, 100). Anal. Calcd for C₃₉H₄₂N₅PtBF₄ (*M_r* = 862.67): C, 54.30; H, 4.91; N, 8.12. Found: C, 54.19; H, 4.76; N, 7.75.

Complex 4 was prepared from *trans*-[Pt(Et₃P)₂Cl₂] (100 mg, 0.199 mmol), 5-ethynyl-2,2'-bipyridine (80 mg, 0.444 mmol), CuI (1.8 mg, 0.009 mmol), in THF (3 mL) and Pr₃NH (2 mL) under strict anaerobic conditions, at RT, during 5 days. During the course of the reaction, a white precipitate formed, and the color of the solution turned from colorless to light-green. After evaporation of the solvent the residue was dissolved in dichloromethane (~50 mL) and washed with water (3 × 50 mL). The organic phase was dried over anhydrous sodium sulfate and filtrated over paper. After rotary evaporation of the solvent, the residue was purified by chromatography on alumina, eluting with CH₂Cl₂-methanol (v/v 99/1) to CH₂Cl₂-methanol (v/v 97/3). Recrystallization by slow evaporation of dichloromethane from a solution containing dichloromethane/cyclohexane afforded crystals of the desired complex **4** as pale yellow crystals (127 mg, 81%). ¹H NMR (300.1 MHz, CD₂Cl₂) δ 8.53 (dm, ³J = 8.0 Hz, 2H), 8.46 (dm, ³J = 8.0 Hz, 2H), 8.28 (dt, ³J = 8.0 Hz, ⁴J = 0.8 Hz, 2H), 8.20 (dd, ³J = 8.0 Hz, ⁴J = 0.8 Hz, 2H), 7.71 (td, ³J = 8.0 Hz, ⁴J = 2.0 Hz, 2H), 7.56 (dd, ³J = 8.0 Hz, ⁴J = 2.0 Hz, 2H), 7.20–7.16 (9 line m, 2H), 2.16 (m, 12H), 1.19 (m, 18H); ¹³C{¹H} NMR (75.1 MHz, CD₂Cl₂+d₆-DMSO (v/v 1/1)): δ 156.4, 155.8, 155.0, 153.2, 150.2, 143.5, 137.5, 124.9, 121.6, 114.9, 99.2, 8.8, 7.6; FT-IR (KBr, cm⁻¹): 2962, 2916, 2870, 2116 (ν_{C≡C}), 1722, 1616, 1552, 1467, 1426, 1403, 1368, 1260, 917, 846, 738; ES-MS *m/z* (nature of the peak, relative intensity): 791.0 ([M+H]⁺, 100). Anal. Calcd for C₃₆H₄₄N₄P₂Pt (*M_r* = 789.79): C, 54.75; H, 5.62; N, 7.09. Found: C, 54.56; H, 5.35; N, 6.93.

Complex 5. In a mixture of dichloromethane (30 mL) and triethylamine (3 mL), Pt(dbbpy)Cl₂ (0.050 g, 0.094 mmol) and 4-ethynyl-2,2'-bipyridine (0.050 g, 0.280 mmol) were successively added. The solution was degassed by bubbling argon through the solution. The addition of CuI (0.001 g, 6 mol %) to the slightly yellow solution resulted in a progressive color change to yellow deep. After stirring at RT for one night, the solvent was removed under reduced pressure, and the residue was purified by column chromatography on alumina. The desired complex

(yellow band) was eluted with a gradient of methanol (0–3%) in dichloromethane as mobile phase. The analytically pure complex was obtained by crystallization in a mixture dichloromethane/hexane (0.065 g, 85%). ¹H NMR (400.1 MHz, d²-dichloromethane): δ 9.64 (d, ³J = 5.7 Hz, 2H), 8.79 (dd, ³J = 2.2 Hz, ⁴J = 0.7 Hz, 2H), 8.67–8.66 (8 line, m, 2H), 8.44 (td, ³J = 7.9 Hz, ⁴J = 0.7 Hz, 2H), 8.37 (dd, ³J = 8.1 Hz, ⁴J = 0.9 Hz 2H), 8.06 (d, ³J = 1.8 Hz, 2H), 7.88 (dd, ³J = 8.1 Hz, ⁴J = 2.0 Hz, 2H), 7.83 (dt, ³J = 7.8 Hz, ⁴J = 1.8 Hz 2H), 7.70 (dd, ³J = 6.1 Hz, ⁴J = 1.8 Hz, 2H), 7.32 (dd, ³J = 4.7 Hz, ⁴J = 1.1 Hz, 1H), 7.30 (dd, ³J = 4.7 Hz, ⁴J = 1.1 Hz, 1H), 1.49 pm (s, 18H). ¹³C{¹H} NMR (100.6 MHz, d²-dichloromethane) δ 165.1, 157.1, 156.9, 153.0, 152.9, 151.6, 149.9, 140.0, 137.5, 125.8, 125.7, 124.1, 121.5, 120.7, 120.2, 99.4, 94.4, 36.7 ppm. FT-IR (ATR): ν = 3046 (m), 2965 (s), 2110 (s, ν_{C≡C}), 1617 (m), 1585 (m), 1568 (m), 1541 (m), 1454 (s), 1432 (m), 1417 (m), 1363 (m), 1251 (m), 1216 (m), 847 (m), 796 (m), 747 (m). ESI-MS (CH₃CN) *m/z* 822.3 ([M + H]⁺). Anal. Calcd for C₄₂H₃₈N₆Pt (*M_r* = 821.87): C, 61.38; H, 4.66; N, 10.23. Found: C, 61.19, H, 4.42, N, 10.02.

Titration of 1 with Fe(ClO₄)₂. A 297 μM solution of Fe(ClO₄)₂·6H₂O and a 20.4 μM solution of **1** were prepared in CH₂Cl₂. The absorption and emission spectra were recorded simultaneously after each addition of Fe^{II}. The titration was considered complete after no additional changes were observed in the absorption and emission properties. All emission spectra and intensity decays were measured using the lowest energy isosbestic point available in the absorption spectrum.

Titration of 1 with Zn(ClO₄)₂. For this experiment, a 299 μM solution of Zn(ClO₄)₂·6H₂O and a 8.81 μM solution of **1** were prepared in CH₂Cl₂. Absorption and emission spectra were measured after each addition of Zn^{II}, and the titration was considered complete when the spectral changes remained constant upon the addition of further aliquots. All emission spectra and intensity decays were measured using the lowest energy isosbestic point available in the absorption spectrum.

Spectroscopic Measurements. UV–vis absorption spectra were measured with a Cary 50 Bio spectrophotometer accurate to ± 2 nm. Uncorrected luminescence spectra measured at room temperature and 77 K were recorded on a PTI Instruments spectrofluorimeter (QM-4/2006-SE) equipped with a 75 W Xe lamp as excitation source and a R-928 PMT detector for the UV–vis region. For detection of singlet oxygen in the near-IR region, a Coherent Innova 306 Ar-ion laser was used as the excitation source in conjunction with a Peltier cooled InGaAs detector with lock-in amplification; the detector was mounted to the exit port of a second monochromator integrated into the PTI system. All the photophysical experiments were performed using optically dilute solutions (OD = 0.08–0.1) in spectroscopic grade solvents, and the samples contained in 1 cm² anaerobic quartz cells (Starna Cells) were deoxygenated with solvent-saturated argon for at least 45 min prior to measurement. For the detection of singlet oxygen, the samples were purged with pure O₂ gas for 2 min prior to data acquisition. Emission lifetimes were measured by means of a nitrogen pumped broadband dye laser (2–3 nm fwhm) (PTI GL-3300 N₂ laser, PTI GL-301 dye laser, C-450 dye) using the experimental apparatus previously described.²⁵ Relative photoluminescence quantum yields were determined using [Ru(bpy)₃]²⁺ in argon saturated CH₃CN (Φ_{em} = 0.062) as the quantum counter.⁵⁹

Transient absorption difference spectra were collected on a Proteus spectrometer (Ultrafast Systems) equipped with a 150 W Xe-arc lamp (Newport), a Chromex monochromator (Bruker Optics) equipped with two diffraction gratings blazed for visible and near-IR dispersion, respectively, and Si or InGaAs photodiode detectors (DET 10A and DET 10C, Thorlabs) optically

coupled to the exit slit of the monochromator. As an excitation source, a computer-controlled Nd:YAG laser/OPO system from Opotek (Vibrant LD 355 II) was used operating at 10 Hz and directed to the sample possessing an optical absorbance between 0.4 and 0.6 at the excitation wavelength. The 64 laser shot averaged data was analyzed by Origin 7.5 or 8.0 software. In these experiments, a flow cell was used to avoid decomposition of the sample.

Time-Dependent Theory. The 77 K emission spectra were calculated using the fundamental equation in time-dependent theory.^{60–68}

$$I(\omega) = C\omega^3 \int_{-\infty}^{+\infty} \exp(i\omega t) \left\{ \langle \Phi | \Phi(t) \rangle \exp\left(-i\frac{E_0}{\hbar}t - \Gamma^2 t^2\right) \right\} dt \quad (1)$$

where $I(\omega)$ is the intensity of emission in photons per unit of volume per unit of time at frequency ω , C is a constant, E_0 is the energy difference between the minima of the excited and ground state, and Γ is a damping factor, which comes from the relaxation into other modes and the “bath”.⁶⁰ In eq 1, the total autocorrelation function term $\langle \Phi | \Phi(t) \rangle$ is the overlap between the initial wave packet, Φ , and the time-dependent wave packet, $\Phi(t)$. In a one-coordinate system and with the assumption that the potential surfaces are harmonic, the force constants are kept the same between the ground and excited states, and the transition dipole moment is a constant (Condon approximation), the total autocorrelation function can be calculated by⁶⁰

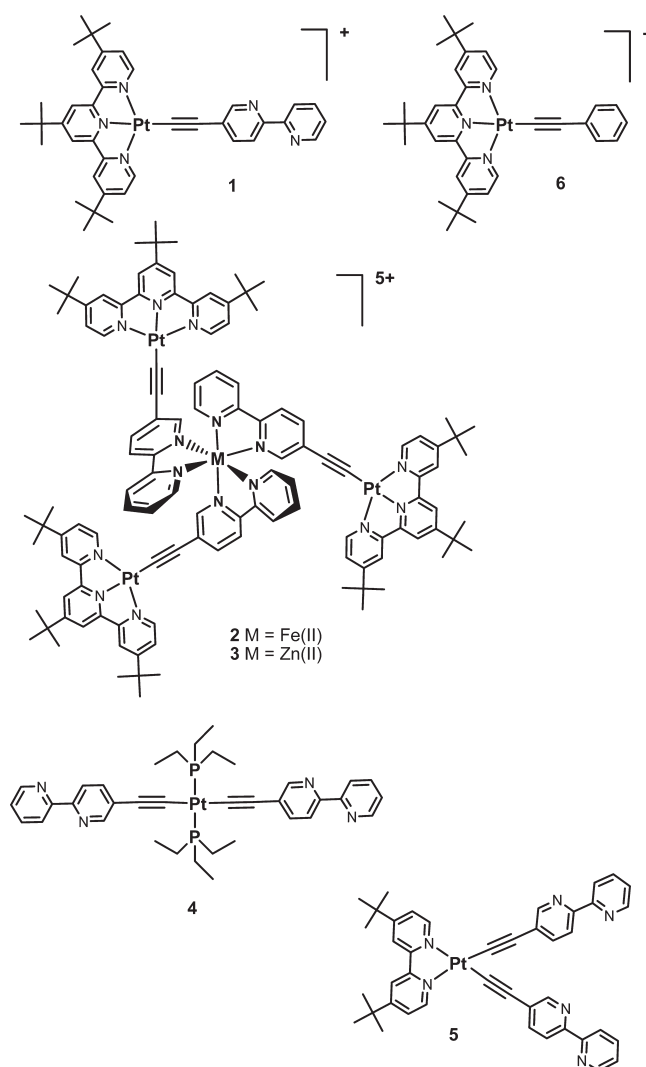
$$\langle \Phi | \Phi(t) \rangle = \exp\left\{-\frac{\Delta^2}{2}(1 - \exp(-i\omega_v t)) - \frac{i\omega_v t}{2}\right\} \quad (2)$$

where ω_v is the vibrational frequency in cm^{-1} and the dimensionless distortion Δ is the displacement of the normal mode. In the current work, ω_v used in the spectra fitting was determined from the vibrational progression measured in the 77 K emission spectra, 1360 cm^{-1} , and the distortion parameter was varied to yield the best fit to the experimental data.

Results and Discussion

Structures. Complexes **1**, **4**, and **5** were synthesized following reported procedures and fully characterized by ^1H and ^{13}C NMR, mass spectroscopy, and elemental analysis. Compound **6** was available from a previous study and chosen as a representative ^3CT model chromophore. The corresponding zinc and iron derivatives were obtained in situ during the titration experiments. As the sample quantities of **1** were somewhat limited, no attempts were made to directly prepare and isolate **2** and **3**. Complexes **1** and **5** display emission emanating from a ^3CT excited state while **4** is an example of a complex with ^3IL parentage. As with other iron(II) polypyridyl complexes, **2** does not display RT photoluminescence. The RT photophysical properties of **3** are consistent with CT

parentage occurring at higher energy relative to parent structure **1**.



Room Temperature Absorption and Photoluminescence.

The absorption and steady-state photoluminescence spectra of compound **1** are displayed in Figure 1. As observed in most other Pt^{II} terpyridyl acetylide complexes, the absorption bands in the region between 250 and 350 nm are assigned to $^1\pi-\pi^*$ transitions localized on the bipyridylacetylide and terpyridyl ligands, and the low-energy absorption band in the visible to charge transfer (CT) transitions; the latter are composed of both ligand-to-ligand and metal-to-ligand components assuming analogous behavior to the closely related model CT structure **6**.^{1,4,12–14,16,17,22} Complex **1** displays an intense broad-band photoluminescence in dichloromethane with $\lambda_{\text{max}} = 575 \text{ nm}$ and a quantum yield of 0.22. The excited state lifetime of complex **1** is $5.8 \mu\text{s}$ (single exponential) at room temperature in degassed CH_2Cl_2 . In coordinative Lewis basic solvents like acetonitrile, a dynamic quenching of the photoluminescence is readily observed. The photophysical data of **1** and **6** are summarized in Table 1. The values of k_r and k_{nr} for **1** and **6** are quantitatively similar, thereby supporting a triplet CT-based parentage for the emitting excited state in **1**. This fact is further

(60) Zink, J. I.; Shin, K.-S. K. In *Advances in Photochemistry*; Wiley-Interscience: New York, **1991**; Vol. 16, pp 119–214.

(61) Lee, S.-Y.; Heller, E. J. *J. Chem. Phys.* **1979**, 71, 4777–4788.

(62) Heller, E. J. *Acc. Chem. Res.* **1981**, 14, 368–375.

(63) Heller, E. J.; Sundberg, R. L.; Tannor, D. J. *J. Phys. Chem.* **1982**, 86, 1822–1833.

(64) Hanna, S. D.; Zink, J. I. *Inorg. Chem.* **1996**, 35, 297–302.

(65) Henary, M.; Wootton, J. L.; Khan, S. I.; Zink, J. I. *Inorg. Chem.* **1997**, 36, 796–801.

(66) Henary, M.; Zink, J. I. *J. Am. Chem. Soc.* **1989**, 111, 7407–7411.

(67) Reber, C.; Zink, J. I. *J. Chem. Phys.* **1992**, 96, 2681–2690.

(68) Wootton, J. L.; Zink, J. I. *J. Phys. Chem.* **1995**, 99, 7251–7257.

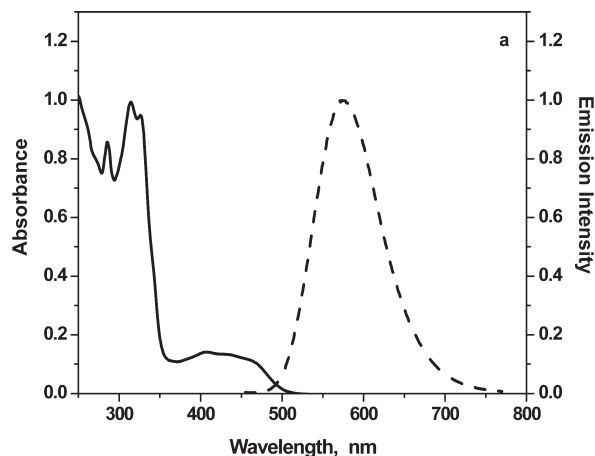


Figure 1. Absorption (solid line) and photoluminescence (dashed line) spectra of compound **1** in CH_2Cl_2 .

confirmed by its susceptibility to dynamic quenching by dissolved dioxygen, ultimately sensitizing $^1\text{O}_2$ photoluminescence in the near-IR at 1270 nm.^{16,17,69,70}

The absorption and steady-state photoluminescence spectra of **4** in CH_2Cl_2 and MTHF are presented in Figure 2. As anticipated from the structure of compound **4**, no CT absorption bands are observed in either solvent system. Only one band near 360 nm is observed corresponding to $\pi-\pi^*$ transitions centered in the $-\text{C}\equiv\text{C}-\text{bpy}$ fragment. The terpyridyl core was replaced by two *trans*-disposed monodentate phosphine ligands to remove any associated MLCT transitions in the metal complex, permitting the study of the photophysics related solely to the bpy-acetylide subunit. Complex **4** displays an intense photoluminescence in degassed dichloromethane, which is significantly quenched in the presence of dissolved dioxygen. The values of k_r and k_{nr} are both 1 order of magnitude smaller than those observed in **1** and **6**, both established as CT-based excited states in nature, Table 1. The combined data support a ligand-centered triplet-based excited state manifold in **4**. Similar results were obtained in MTHF. The emission profile is somewhat structured, with $\lambda_{\text{max}} = 520$ nm and a pronounced shoulder at 555 nm with an excited state lifetime of 26 μs in argon-saturated dichloromethane (23.6 μs in degassed MTHF). As mentioned earlier, the absence of the bpy core guarantees subtraction of the CT transitions, leading to the conclusion that the emission observed in **4** should arise solely from a ligand centered (bpy-acetylide) excited state. On the basis of our previous work in this area and some of the data presented below, we do not believe that the *trans*-disposed bpy-acetylides are in strong electronic communication across the Pt^{II} center.

The photophysical properties of the $^t\text{Bu}_2\text{bpyPt}-(\text{C}\equiv\text{Cbpy})_2$ (**5**) species were also investigated to fully compare and understand the influence of the polydentate platform on the photophysics observed. The absorption and steady-state photoluminescence spectra of **5** in argon-saturated dichloromethane are presented in Figure 3. The bands between 300 and 350 nm are assigned to $\pi-\pi^*$ transitions on the various bpy ligands, and the band at

low energy is assigned to CT transitions ($\lambda_{\text{max}} = 400$ nm), which are blue-shifted relative to the absorption bands observed in the parent terpyridyl complex (**1**). This phenomena has been reported previously in the parent complexes $[(^t\text{Bu}_3\text{tpy})\text{Pt}(\text{C}\equiv\text{CPh})]^+$ and $(^t\text{Bu}_2\text{bpy})\text{Pt}(\text{C}\equiv\text{CPh})_2$, where the CT absorption band of the bpy complex always appears at higher energies than the corresponding CT band of the parent tpy complex.¹ This observation results from more ligand-to-ligand CT participation in the lowest energy optical transitions in the tpy-containing structures. In dichloromethane, complex **5** displays a very intense photoluminescence, $\lambda_{\text{em}} = 525$ nm, which is also quite sensitive to quenching in the presence of oxygen. The excited state lifetime of **5** in argon-saturated CH_2Cl_2 at room temperature is 3.67 μs as ascertained through time-resolved photoluminescence experiments. The broad and structureless emission profile in addition to the values of k_r and k_{nr} (Table 1) are almost identical to those of the closely related parent CT complex, $\text{Pt}(\text{dbbpy})(\text{C}\equiv\text{CPh})_2$.¹⁰ These combined attributes lead us to the conclusion that the photoluminescent excited state in **5** is CT in nature at RT.

Photophysics of the Titration Products. (A). $\text{Fe}(\text{II})$ Titration. As complex **1** has a free chelation site on the pendant bipyridylacetylide unit, attachment of dissolved metal ions is facile and can potentially modify the photophysics of the free base containing Pt^{II} complex. Upon addition of Fe^{II} to a solution of **1** in CH_2Cl_2 , a new band at 542 nm was observed, which was readily assigned to a $\text{Fe}^{\text{II}}-\text{bpy}$ CT transition (Figure 4a).^{17,71,72} Three clearly resolved isosbestic points at 332, 445, and 495 nm were observed in this titration. The CT band corresponding to the original Pt^{II} system blue-shifted upon Fe^{II} coordination, going from 430 to 409 nm, with an incremental increase in its absorbance. Similar to the conclusion drawn in previous work, the observed blue shift in the CT absorption band can be attributed to the fact that upon chelation of Fe^{II} , which is Lewis acidic, the highest occupied molecular orbitals (HOMOs) become stabilized relative to **1**, thereby increasing the energy of the associated transitions.^{17,22,73–75} The absorption bands corresponding to the $\pi-\pi^*$ transitions also increased in intensity upon chelation of **1** to Fe^{II} . Addition of Fe^{II} to a solution of **1** in CH_2Cl_2 induced a static quenching of the emission profile at 575 nm (Figure 4b) suggesting that upon coordination of Fe^{II} , ligand field and other low energy states present in the new polynuclear structure readily affords deactivation of the excited-state presumably through low lying ligand field states. In Figure 4b it is possible to observe that even after the titration equivalence point (0.34 equiv) some weak residual emission remains near 532 nm which corresponds to the emission maximum observed for the Zn^{II} analogue, the titration product designated as **3** whose results are presented

(71) Zigler, D. F.; Elvington, M. C.; Heinecke, J.; Brewer, K. J. *Inorg. Chem.* **2006**, *45*, 6565–6567.

(72) Baitalik, S.; Wang, X.-Y.; Schmehl, R. H. *J. Am. Chem. Soc.* **2004**, *126*, 16304–16305.

(73) Yam, V. W.-W.; Hui, C.-K.; Yu, S.-Y.; Zhu, N. *Inorg. Chem.* **2004**, *43*, 812–821.

(74) Lu, W.; Chan, M. C. W.; Zhu, N.; Che, C. M.; He, Z.; Wong, K. M.-C. *Chem.—Eur. J.* **2003**, *9*, 6155–6166.

(75) Han, X.; Wu, L.-Z.; Si, G.; Pan, J.; Yang, Q.-Z.; Zhang, L.-P.; Tung, C.-H. *Chem.—Eur. J.* **2007**, *13*, 1231–1239.

(69) Mulazzani, Q. G.; D'Angelantonio, M.; Venturi, M.; Rodgers, M. A. *J. Phys. Chem.* **1991**, *95*, 9605–9608.

(70) Bromberg, A.; Foote, C. S. *J. Phys. Chem.* **1989**, *93*, 3968–3969.

Table 1. Photophysical Properties of Compounds 1 and 4–6

compound	λ_{abs} , nm	λ_{em} , nm	E_{00} (77 K), cm^{-1}	Φ_{em}^c	$\tau_{\text{em}},^c \mu\text{s}$	$\tau_{\text{TA}}, \mu\text{s}$	$k_{\text{nr}}^d (\times 10^5) \text{ s}^{-1}$	$k_r^e (\times 10^4) \text{ s}^{-1}$
1	286, 315, 326, and 430 ^a	575 ^a ; 512, and 549 ^b	19500 (19530) ^h	0.22	5.79 ^a ; 31.1 ^b	5.7	1.35	3.80
4	360 ^a ; 354 ^g	520 and 555 ^a ; 518 and 555 ^f ; 510 and 548 ^b	19550 (19608) ^h	0.12	26 ^a ; 23.6 ^f ; 184 ^b	20	0.338	0.462
5	321, 337, and 400 ^a	527 ^a ; 507 and 542 ^b	19750 (19724) ^h	0.56	3.67 ^a ; 88 ^b	3.6	1.20	15.2
6	315, 340, 411, and 458 ^a	592 ^a		0.15	3.8 ^a	3.0	2.20	3.90

^a Measured in Ar saturated CH_2Cl_2 solution at room temperature. ^b Measured at 77 K in an EtOH/MeOH 4/1 matrix. ^c Photoluminescence quantum yields and lifetime decays, $\pm 5\%$. ^d $k_{\text{nr}} = (1 - \Phi)/\tau$. ^e $k_r = \Phi/\tau$. ^f Measured in Ar saturated MTHF solution at room temperature. ^g Determined through fitting the 77 K emission profile by time-dependent theory, see text for details. ^h Highest energy peak in the 77 K emission spectrum.

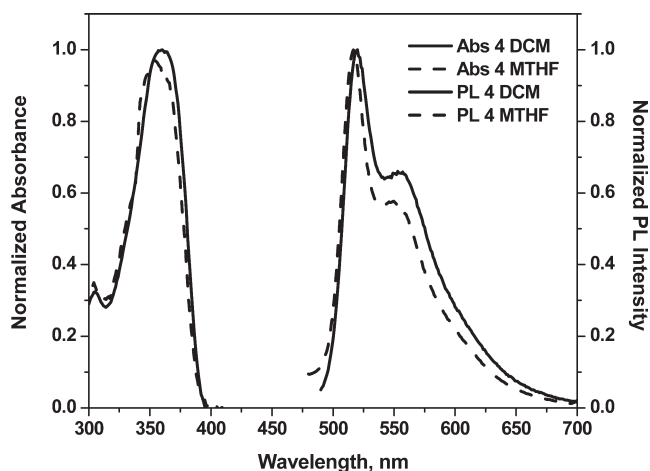


Figure 2. Absorption and photoluminescence spectra of 4 in CH_2Cl_2 (solid line) and in argon-saturated MTHF (dashed line) at room temperature.

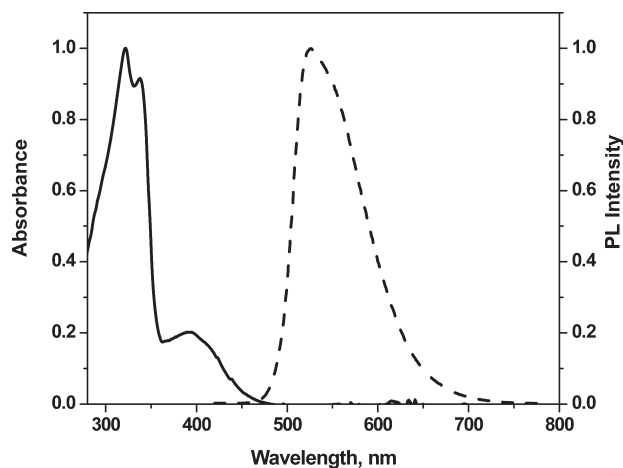


Figure 3. Absorption (solid line) and photoluminescence (dashed line) spectra of 5 measured in argon-saturated CH_2Cl_2 at room temperature.

below. It was not possible to determine the excited state lifetime of this residual emission observed because it was shorter than the instrument response function, < 15 ns. No absorption transients could be resolved for 2 within the IRF of our nanosecond laser flash photolysis apparatus.

(B). Zn(II) Titration. To determine how the coordination of the pendant bipyridyl unit affects the energy levels of the resultant complex, the same titration experiment presented above was also performed with Zn^{II} ; this presents the octahedral coordination environment of Fe^{II} without the corresponding low energy ligand field

deactivating states. Upon addition of Zn^{II} , the CT band of complex 1 blue-shifted, increasing its intensity at 412 nm (Figure 5a), similar to the behavior observed upon addition of Fe^{II} . The blue shift is again attributed to the Lewis acidity of Zn^{II} which in essence stabilizes the HOMO levels relative to the “free” bpy complex 1. We note that an identical blue shift was observed when excess HClO_4 was added to a CH_2Cl_2 solution of 1, thereby simulating the influence of acid on the nonbonding electrons resident on the bpy-acetylide nitrogens (Figure 6). This is identical to the behavior observed in the molecule containing the pendant tpy unit and also has been observed previously in analogous amine-substituted acetylide complexes of Pt^{II} .^{73–75} As expected from the electrochemical inaccessibility of the Zn^{II} metal center, no additional CT bands were generated in the absorption spectrum during the titration, and the formation of two isosbestic points at 334 and 446 nm were observed (Figure 5a). Even though quenching of the emission at 575 nm was observed throughout the titration experiment, the new ZnPt_3 complex (3) formed was emissive under the conditions used, with $\lambda_{\text{max}} = 532$ nm and an isoemissive point at 551 nm, Figure 5b. During the titration, it was rather straightforward to visualize how the emission band of the new complex increased as the titration proceeded rendering a new profile that is highly sensitive to the presence of dissolved oxygen. In a related control experiment, the addition of excess HClO_4 to 1 produces an emission profile blue-shifted relative to the free base but red-shifted with respect to the ZnPt_3 titration product, Figure 6. While it is clear that stabilization of the HOMO level(s) result upon coordination to Zn^{II} as well as upon protonation, interaction of 1 with these two cations results in significantly measurable differences in the photophysical properties of 3 and protonated 1. The combined photophysical data for titration product 3 and protonated 1 are collected in Table 2.

The luminescence quantum yield of titration product 3 is 0.24, and the excited state luminescence intensity decay yields a single exponential time constant of 16.9 μs in CH_2Cl_2 at room temperature, representing a 2.9-fold excited state lifetime enhancement relative to 1. This result is very similar to the report from Barigelletti et al. on Ru^{II} terpyridyl complexes with pendant free base tpy ligands, with the exception that they observed bathochromic shifts in the absorption/emission spectra of their Zn^{II} coordinated complexes.^{76,77} In complex 3, the observed

(76) Barigelletti, F.; Flamigni, L.; Calogero, G.; Hammarstroem, L.; Sauvage, J.-P.; Collin, J.-P. *Chem. Commun.* **1998**, 2333–2334.

(77) Barigelletti, F.; Flamigni, L.; Guardigli, M.; Sauvage, J.-P.; Collin, J.-P.; Sour, A. *Chem. Commun.* **1996**, 1329–1330.

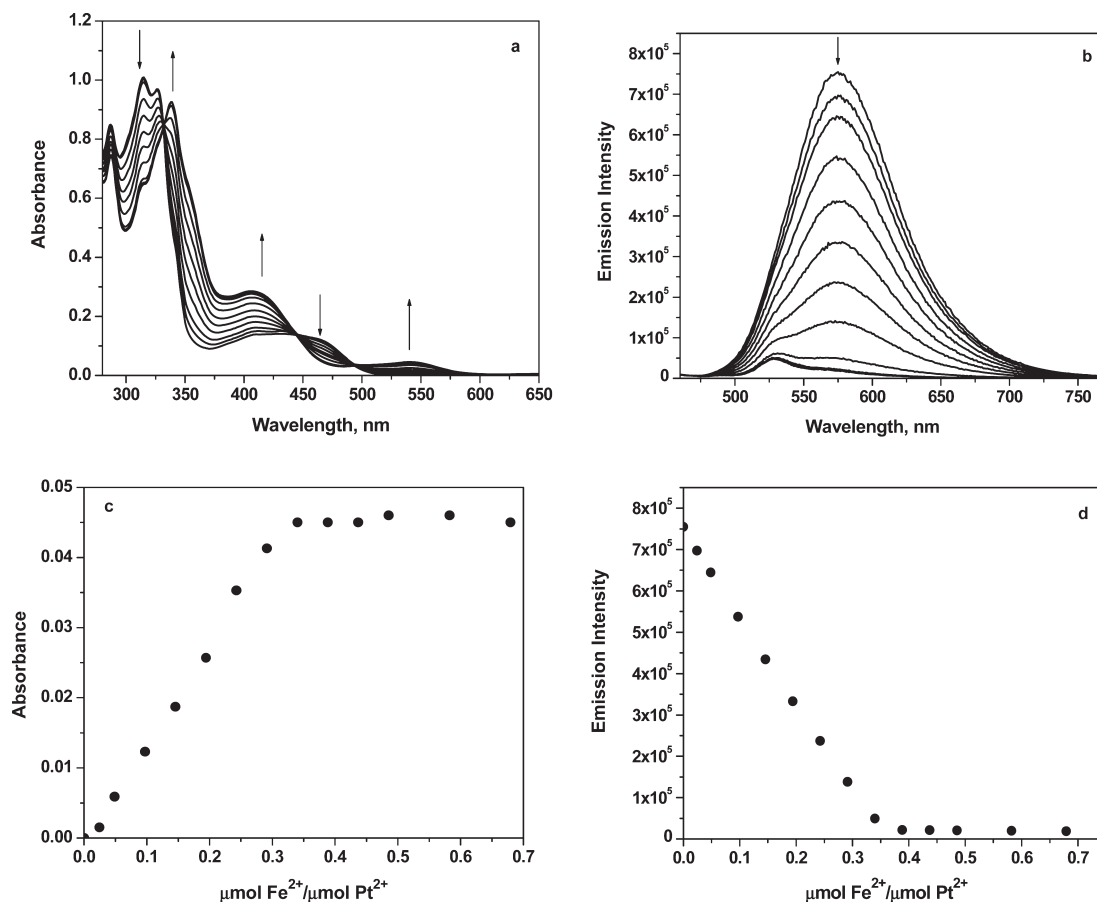


Figure 4. Titration of **1** with Fe^{II} followed by absorption (a) and photoluminescence (b) changes in CH_2Cl_2 . Changes in absorbance at 540 nm (c) and emission at 575 nm (d) as function of $\mu\text{mol of Fe}^{\text{II}}/\mu\text{mol of Pt}^{\text{II}}$. No further spectroscopic changes were observed beyond 0.34 equiv (stoichiometric point) of Fe^{II} added.

blue shifts in the absorption/emission spectroscopy can be rationalized in terms of stabilization of the HOMO levels, rendering a higher energy CT species with respect to the free base **1**. Qualitatively, the lack of a highly structured emission profile in **3** suggests that the photoluminescence is not likely ligand-centered in nature. Nonetheless, the parentage of this excited state cannot be definitively assigned solely on the basis of RT photoluminescence data, and transient absorption difference spectra are presented below.

The photophysics of the Zn^{II} analogue of **4** were measured as well. However, the presence of two chelation sites in **4** appears to render a complex coordination polymer structure upon coordination of Zn^{II} . Chelation of Zn^{II} induces a red shift in the absorption band maximum ($\lambda_{\text{abs}} = 393 \text{ nm}$), Supporting Information, Figure S1, consistent with the planarization of the two bipyridyl acetylide units, which increases the conjugation length parallel to the long molecular axis. The new conformation(s) may introduce ligand-to-ligand charge transfer (LLCT) transitions, making difficult direct comparisons with the photophysics emanating from **3**. In any case, the photoluminescence spectrum of **4** in the presence of $\text{Zn}(\text{II})$ is broad and red-shifted relative to **4** ($\lambda_{\text{em}} = 567 \text{ nm}$) with a corresponding excited state lifetime of $47.7 \mu\text{s}$. Since the emission lifetime is significantly extended in relation to free base **4** (with a concomitant red shift of the spectrum), we conclude that more extended

π -conjugation in the bipyridylacetylide ligand produces lower energy ligand-localized phosphorescence in this instance. Interestingly, the bipyridyl-based CT model chromophore **5** displays quite similar photophysical behavior upon $\text{Zn}(\text{II})$ coordination, Supporting Information, Figure S2. We believe that in these more complex polynuclear systems, the lowest excited state at RT is best described as ligand-localized, but with more extended π -conjugation relative to that observed in the free bases **1**, **4**, and **5** at 77 K.

Nanosecond Transient Absorption Spectroscopy. To elucidate and precisely conclude the true nature of the emissive states involved in the excited states of **1** and **3** at RT, transient absorption measurements were performed on both molecules, Figure 7. The normalized transient absorption difference spectra presented in Figure 7 are emission corrected as both complexes exhibit long-lived (and strong) photoluminescence in degassed solutions. All the transients display long-lived excited state decays consistent with a triplet-excited state parentage, which agree well with the corresponding photoluminescence data, see Tables 1 and 2. The transient absorption difference spectrum of **1** exhibit features that resemble what is typically observed for complexes with ^3CT excited states (Figure 7a).^{4,20} A representative example of a related CT complex is **6** whose transient absorption features have been studied previously,⁴ and are superimposed here for comparative purposes. In degassed CH_2Cl_2 , **6** displays

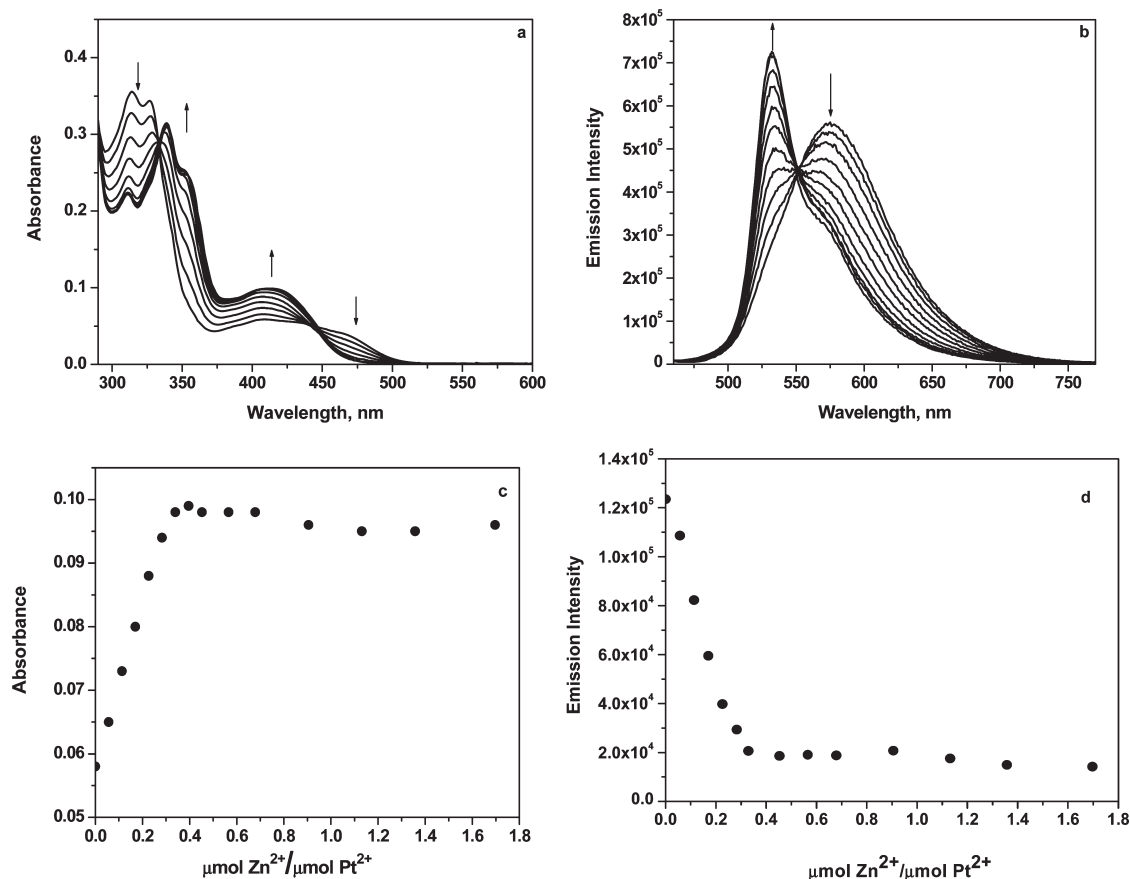


Figure 5. Titration of **1** with Zn^{II} followed by absorption (a) and photoluminescence (b) changes in CH_2Cl_2 . Changes in absorbance at 407 nm (c) and emission at 600 nm (d) as function of $\mu\text{mol of Zn}^{\text{II}}/\mu\text{mol of Pt}^{\text{II}}$. No further spectroscopic changes were observed beyond 0.33 equiv (stoichiometric point) of Zn^{II} added.

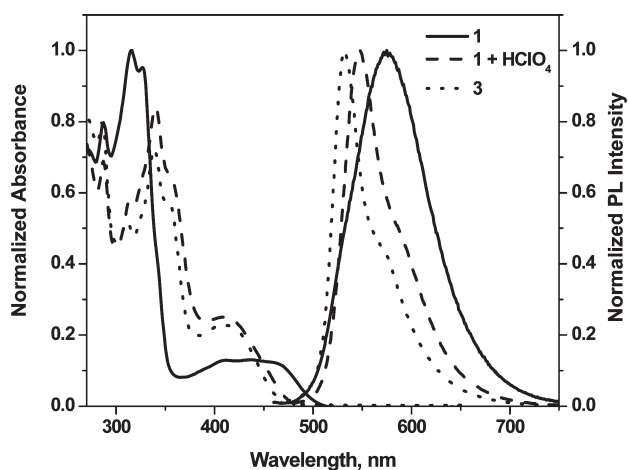


Figure 6. Comparison of the absorption and emission profiles of compounds **1** (solid line), **3** (dotted line), and the product of the acid titration of **1** with excess HClO_4 (dashed line) measured in degassed CH_2Cl_2 .

positive transient absorption features in the 500–550 nm region and a broadband between 600 and 1200 nm, which has been assigned to the photogenerated hole delocalized across the Pt center and the ancillary acetylide ligand.⁴ In Figure 7a similar features, yet blue-shifted in comparison, are observed for the transient generated in **1**, with absorptions between 460 and 550 nm and a more intense band in the 580–1140 nm region along with additional non-descriptive features extending into the near-IR. With

the combination of photoluminescence and transient absorption experiments it is possible to conclude that the excited state in **1** at RT is indeed ^3CT in nature.

Complex **3** exhibits a quite distinct transient absorption difference spectrum with respect to **1** and **6** (Figure 7), producing a broad positive transient absorption that extends from 415 to 1100 nm. The transient absorption excited state lifetime in **3** also quantitatively agrees with that measured by time-resolved photoluminescence, so the absorption transients are definitely reporting on the same species producing the long-lived photoluminescence. The transient absorption difference spectrum of **4** was recorded to establish the transient features associated with the ligand-localized (bpy-acetylide) excited state at RT. This complex was extremely unstable in CH_2Cl_2 under the same experimental conditions used in the data acquisition of **1** and **3**. For this reason, the TA difference spectrum of **4** was measured in MTHF. The difference spectrum of **4** is indeed markedly different from the TA spectra recorded for **1** and **6** yet is also rather distinct with respect to **3**. The excited state lifetime of the transients in **4** (20 μs) is reasonably consistent with the photoluminescence-determined lifetime measured above. The ligand-localized transient species in **4** displays one absorption maximum at 400 nm and a broader band centered at 600 nm. The difference spectrum of this complex also displays positive absorptions in the near-IR region with intensities that are significantly attenuated in relation to its corresponding features observed in the visible. While the TA

Table 2. Photophysical Properties of the Titration Products

compound	λ_{abs} , nm	λ_{em} , nm	Φ_{em}^c	τ_{em}^c , μs
2	286, 339, 409, and 542 ^a			
3	286, 339, and 413 ^a	532 and 569(sh) ^a ; 516 and 554 ^b $E_{00} = 19380 \text{ cm}^{-1}$ ^e	0.24	16.9 ^a ; 73.6 ^b
1 + HClO₄	289, 339, and 413 ^d	547 and 590(sh) ^d ; 506 and 541 ^b		14.7 ^d ; 31.8 ^b

^a Measured in Ar saturated CH_2Cl_2 solution at room temperature. ^b Measured at 77 K in an EtOH/MeOH 4/1 matrix. ^c Photoluminescence quantum yields and lifetime decays, $\pm 5\%$. ^d Measured after an excess of HClO_4 was added to an Ar-saturated CH_2Cl_2 solution of **1** at room temperature. ^e Determined through fitting the 77 K emission profile by time-dependent theory, see text for details.

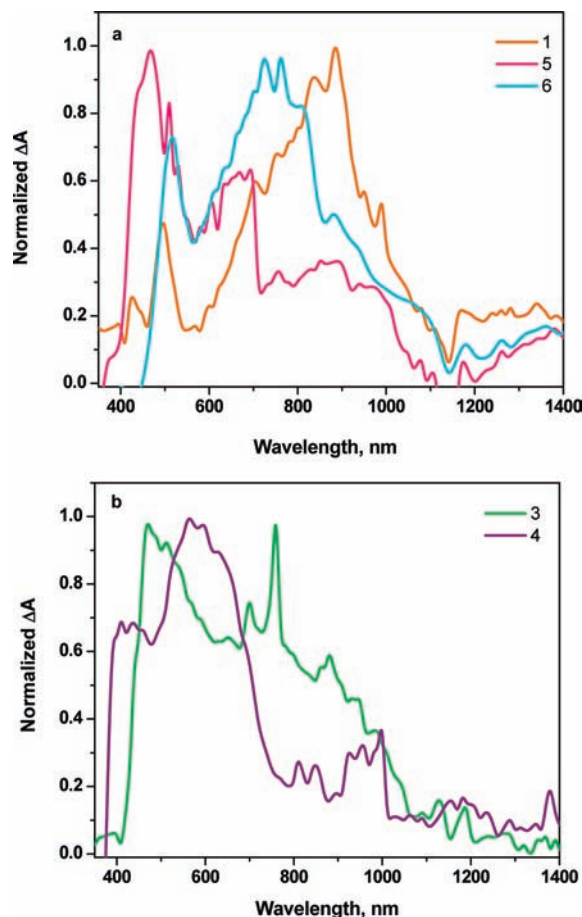


Figure 7. Selected normalized transient absorption difference spectra of **1**, **5**, and **6** (a) and **3** (b) measured in degassed CH_2Cl_2 following a 5–7 ns 420 nm laser pulse. Selected transient absorption difference spectrum of **4** (b) measured in degassed MTHF following a 355 nm laser pulse. The delay time presented is 0.100 μs for all chromophores.

difference spectra clearly demonstrate that the lowest excited state in **1** and **4** are distinct, ^3CT in the former and ^3IL in the latter, the nature of the lowest excited state in **3** (at RT) remains somewhat ambiguous. Since the TA difference spectrum of complex **3** does not directly coincide with the corresponding difference spectrum of **4**, which certainly possesses a ligand-centered parentage, we are forced to conclude that the RT excited state in **3** is more consistent with a ^3CT excited state manifold.

The TA difference spectrum of **5** measured in argon-saturated CH_2Cl_2 is also displayed in Figure 7a. The prominent transients include an absorption band centered at 466 nm and a second band centered around 670 nm. This complex also displays a broadband in the near IR region, ranging from 730 nm to ~ 1060 nm. The closest CT analogue to complex **5**, structurally speaking,

is $(^t\text{Bu}_2\text{bpy})\text{Pt}(\text{C}\equiv\text{CPh})_2$. Its TA features have been reported, and it is well-known that this complex belongs to the family of complexes that display a CT excited state.^{19,20} The $(^t\text{Bu}_2\text{bpy})\text{Pt}(\text{C}\equiv\text{CPh})_2$ complex displays a positive transient absorption across the entire spectral range investigated (350–1400 nm), with bands at 450 and 620 nm and a lower energy broadband that begins around 800 nm and expands into the near-IR. The TA difference spectrum of **5** also differs from the TA spectrum recorded for the model complex **4**. In general, the photophysical properties recorded for **5** at RT appear to be more consistent with a ^3CT parentage, but the differences observed in the difference spectra between **5** and the phenylacetylide parent complex, $\text{Pt}(\text{dbbpy})(\text{C}\equiv\text{CPh})_2$, indicate that the excited states in both molecules differ. It is well-known that the HOMO level in this type of complex draws contributions from both the metal center and the acetylide ligand. It is possible that the $-\text{C}\equiv\text{C}-\text{bpy}$ fragment presents a distinct electronic influence relative to phenylacetylide, rendering a complex with a larger LLCT contribution, leading to the differences observed in the TA difference spectra. Also, the excited state lifetime of **5** is significantly longer compared to that of the phenylacetylide analogue (3.67 μs vs 1.2 μs), indicating significant electronic differences leading to distinct excited state decay.

77 K Photoluminescence. Tables 1 and 2 contain all of the relevant 77 K photophysical data for the compounds in this study along with their measured and fitted (time-dependent theory) E_{00} values. We note that the E_{00} values vary by less than 400 cm^{-1} across the entire series of molecules. Figure 8a displays the emission spectra recorded for **1**, **3**, and protonated **1** at 77 K. Each complex displays a vibronically structured emission profile in the 4:1 EtOH/MeOH glassy matrix with a concomitant blue shift in their emission bands relative to those observed at room temperature. The vibrational spacing of $1300\text{--}1400 \text{ cm}^{-1}$ observed at 77 K (Figure 8a) is consistent with the vibrational modes on one of the polyimine aromatic systems (largely $\text{C}=\text{C}$ and $\text{C}=\text{N}$ in nature), which presents the possibility of a ligand localized emission at 77 K.^{5,12} Ligand-centered bpy-acetylide based phosphorescence is believed to emanate from **4** at both RT and 77 K, the latter is presented in Figure 8b. The spectral profile and lifetime of **4** at 77 K ($\tau = 184 \mu\text{s}$) leaves little doubt that the excited state involved in the photoluminescence is indeed ligand-centered on the bpy-acetylide framework. The striking similarities in the 77 K emission spectra of complexes **1**, **3**, protonated **1**, and **4** suggest that the excited state at low temperature in these complexes is the same, i.e., a bipyridylacetylide localized triplet state. However, the emission spectra of all these complexes do not perfectly align energetically at 77 K, and the excited

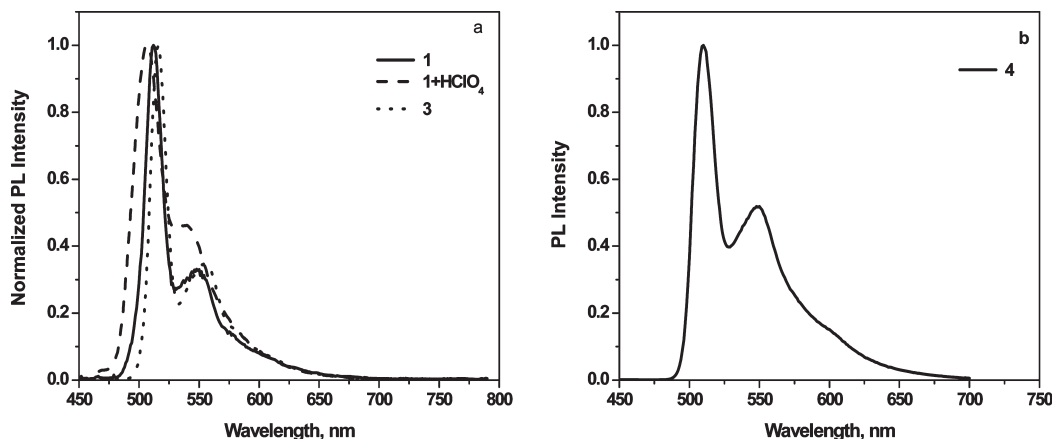


Figure 8. (a) Comparison of the normalized emission profiles of **1** (solid line), **3** (dotted line), and protonated **1** (dashed line) in 4:1 EtOH/MeOH matrixes at 77 K. (b) Photoluminescence spectra of **4** measured in a 4:1 EtOH/MeOH matrix at 77 K.

state lifetimes in **1**, **3**, and protonated **1** are each attenuated with respect to **4** suggesting strong electronic influence being imparted by the CT manifold at low temperature, see Tables 1 and 2. Such configuration mixed excited states can be produced at 77 K resulting from small energetic differences between charge transfer and ligand-localized triplet manifolds.^{1,19,78,79} The net result is what is observed here, the emission in **1**, **3**, and protonated **1** appears to be bpy-acetylide based but possesses excited state lifetimes shorter than the “pure” bpy-acetylide-based phosphorescence measured in **4**. Similar observations were revealed for the bipyridyl analogue **5** whose 77 K emission can best be described as configuration mixed, Supporting Information, Figure S3.

Conclusions

We have demonstrated that the title Pt^{II} complex presented here is not suitable for the production of long-lived Fe^{II}-containing transition metal complexes. On the other hand, chelation of Zn^{II} to the pendant unit in **1** demonstrated that it is possible to go from a mononuclear system displaying emission from a ³CT excited-state manifold (**1**) to a tetra-nuclear complex (**3**) possessing a higher energy excited state with higher energy absorption features, longer excited state lifetime, and higher quantum efficiency with CT parentage. The TA data obtained for **1** clearly indicates that the lowest excited state in this molecule possess a CT parentage as it has been reported for the parent model complex **6**; these transients are quite distinct with respect to those acquired for the bpy-acetylide ligand localized triplet state in model chromophore **4**. The absorption transients measured for **3** are clearly different from **4** which rules out the possibility of a ligand localized excited state in the ZnPt₃ complex. The combined photophysical data suggests that the ZnPt₃ (**3**) titration product possesses a lowest CT excited state which happens

to reveal itself at higher energies with a longer excited state lifetime relative to the free base **1**. Combined photoluminescence and transient data obtained for **5** reinforced the conclusion that the lowest emitting state in this molecule certainly possesses a CT parentage at RT. At low temperature, **1** and **3** displayed structured emission profiles, which are consistent with a ligand-based (bpy-acetylide) parentage of the emitting state, as appropriately modeled by **4**. However, the differences in the lifetimes indicate that the excited states in **1** and **3** are somewhat distinct at low temperature, and compared to the low temperature photophysics observed for **4**, leads to the conclusion that the energetically proximate ³CT state produces excited state lifetimes shorter than expected for a “pure” ligand-centered triplet phosphorescence. At 77 K, the large increase of the lifetime in **5** seems to indicate that the photoluminescence is also dominated by a ligand-centered excited state. However, the lifetime observed for **5** at low temperature is definitively shorter than that of model complex **4** whose excited state parentage is undoubtedly ligand localized. This latter result suggests that at 77 K, the electronic influence of the CT manifold in **5** persists, similar to that observed in **1** and **3**.

Acknowledgment. F.N.C. acknowledges support from the Air Force Office of Scientific Research (FA9550-05-1-0276), the National Science Foundation (CHE-0719050 and CBET-0731153), and the BGSU Research Enhancement Initiative. Funding from the ANR FCP-OLEDs N°-05-BLAN-0004-01 (R.Z.) is acknowledged. We are indebted to Prof. Francesco Barigelli (Istituto FRAE-CNR, Bologna, Italy) for helpful discussions and to Prof. Jeffrey I. Zink at UCLA for providing the necessary programs enabling our use of the time-dependent theory for emission spectral fitting.

Supporting Information Available: Additional photoluminescence spectra and 77 K emission spectral fitting from time-dependent theory. This material is available free of charge via the Internet at <http://pubs.acs.org>.

(78) Crosby, G. A. *Acc. Chem. Res.* **1975**, *8*, 231–238.

(79) Watts, R. J.; Crosby, G. A. *Chem. Phys. Lett.* **1972**, *13*, 619–621.